J. Biochem. 125, 422-429 (1999)

Molecular Structure of the Amyloid-Forming Protein kappa I Bre[1]

L.K. Steinrauf,*,†,2 Michael Y. Chiang,‡ and David Shiuan†

*Department of Biochemistry and Molecular Biology, Indiana University School of Medicine, Indianapolis, Indiana, USA; and †Department of Biological Sciences, and ‡Department of Chemistry, National Sun Yat-sen University, Kaohsiung 80424, Taiwan

Received September 25, 1998; accepted November 28, 1998

The molecular structure of the amyloid-forming Bence-Jones protein kappa I Bre has been determined by X-ray crystallography at 2.0 Å resolution. The fragment from the kappa chain of immunoprotein contains 107 amino acid residues, and polymerizes in the crystal form into a giant helical spiral, surrounding a cylinder of water 50 Å in diameter with a repeat of 77.56 Å, containing 12 kappa molecules, plus another 12 molecules from neighboring parallel spirals. The resulting structure has many features which have been found or suggested from studies on the protein fibrils found in amyloid deposits. From the results of the X-ray crystal structure a hypothesis is presented for the structure and formation of the amyloid fibril.

Key words: amyloidosis, Bence-Jones protein, fibril model, X-ray crystallography.

Amyloidosis, as described in a recent review (*1*), is a disorder in which extra-cellular deposits of protein-based material accumulate in organs, ultimately leading to the destruction of organ function and often to the death of the patient. There are several proteins which are known to produce amyloid deposits in man, and amyloidosis probably exists in other animals as well. Most of the mass of the amyloid deposit consists of insoluble fibrils made up mostly of a single protein species, one that normally is found circulating in the blood. Historically, amyloid deposits were identified by the similarity to amylose by histochemical staining (Virchow, R., 1851. See Ref. *1*) until the 1920s when the staining by Congo red (*2*), which would exhibit green fluorescence under the polarizing microscopy (*3*), became used.

The fibrils of amyloid deposits have been described by the electron microscopic studies of Cohen and Calkins (*4*) as being composed of non-branching rods or cylinders of protein material with a diameter of 70 to 100 Å and of variable length, with the peptide chain perpendicular to the fiber axis. Eanes and Glenner (*5*) deduced from the X-ray diffraction that the proteins are arranged in a cross-pleated β-sheet conformation and suggested that the polypeptide backbones were perpendicular to the long axis of the fibril. The fibrils are not perfectly straight, but often have a slight wobble, and occasional bulges are seen along the length. Analysis of the infrared spectra is consistent with the association of the polypeptide chains to be antiparallel (*6*).

Because of the insolubility (*7*), amyloid fibrils are particularly resistant to chemical and physical analysis. The amyloid deposits start forming as a consequence of another disorder or disease (trauma, diabetes), or may be inherited (such as familial amyloidogenic polyneuropathy, FAP (*8*), and in at least some forms of Alzheimer's disease), in which case the protein in the fibrils may be a mutation. The amyloid may invade many of the vital organs or be restricted to only one organ, such as the central nervous system in the case of Alzheimer's disease (*1*).

The best studied case is that of FAP (*8*), which is caused by a single base mutation of the blood protein, transthyretin, TTR. Transthyretin, formerly known as prealbumin, circulates in the blood as a tetramer, and transports the hormone thyroxin and the retinol-carrier protein complex using separate binding sites on the tetramer. The molecular structure of TTR was one of the very early successes of X-ray crystallography, being preceded only by myoglobin, hemoglobin, and lysozyme. The TTR structure, presented by Blake *et al.* in 1978 (*9*), has since been determined with much greater accuracy by Hamilton *et al.* (*10*). Two of the nearly 30 known lethal mutations of TTR have now been determined by X-ray crystallography, the Val30Met and the Leu82Ser by Hamilton *et al.* (*10-12*). The X-ray crystal structure of a benign variant, Ala109Thr, determined by Steinrauf *et al.* (*13*), showed that TTR could have a mutation at an interior site without becoming amyloidogenic.

The Bence-Jones proteins are another type that is associated with amyloid. Bence-Jones proteins are the N-terminal part of the lambda or kappa light chain gamma globulin. In certain disorders these are found in large amounts in the blood and urine (*1*).

The structure determination of Bre was first presented at the annual meeting of the American Crystallographic Association, by Steinrauf *et al.* (*14*). A preliminary description of the crystal structure and some discussion of the amyloid fibril model was published by Schormann *et al.* (*15*).

The study of amyloidogenic proteins by X-ray crystallography has two objectives. The first is to understand better

[1] Support for this work has been provided by grants NSC 87-2622-B110-001 and NSC 87-2311-B110-008 from the National Science Council, Republic of China.

[2] To whom correspondence should be addressed. E-mail: lsteinra@www.ora.nsysu.edu.tw

the altered properties of the protein in the prefibril state. Why does the prefibril protein become unstable, and what can prevent the fibril formation? The second is to obtain, indirectly, information about the nature of the amyloid fibrils in order to suggest methods to prevent or reverse the formation.

MATERIALS AND METHODS

Protein Preparation and Purification—The protein Bre was obtained as described previously (*15*). The protein was first isolated from the urine of a patient. Recombinant protein was produced by *Escherichia coli* from the patient's DNA as described previously (*15*). Briefly, DNA was obtained from bone marrow cells of the patient, and the oligonucleotide primers were constructed from the amino acid sequence of Bre and published sequences of the signal peptide for κI proteins. The PCR amplified product was ligated into pCA11 and used to transform *E. coli* strain HB101. Cells containing the desired plasmid were then grown in TY broth. After growth the cells were centrifuged and lysed by freeze/thawing and sonication. The Bre protein was then purified on DEAE cellulose.

Crystallization—About 50 μl of a 10 mg/ml solution were used in a variety of crystallization conditions with the only success coming from high concentrations of ammonium sulfate in citrate buffer. Two crystals, rods with hexagonal cross section, of usable size, 0.2×0.3 mm were obtained from 60% ammonium sulfate, 200 mM citrate, pH 5.4.

Data Collection—Data were collected on one crystal using the Rigaku Raxis II image plate detector. Although the appearance of the crystal suggested hexagonal symmetry, data for 180° of rotation were measured. Attempts to reduce the data to a hexagonal system were unsuccessful, giving an R_{merge} of 36%. The data were therefore reduced as

TABLE I. **Data collection and refinement.**

Space group	$P2_1$	$C222_1$
Cell dimensions	a=82.56 Å	a=143.99 Å
(in Ångstrom units)	b=82.66 Å	b=82.66 Å
	c=77.56 Å	c=77.56 Å
	γ=120.0°	
Data collector	Rigaku Raxis II	
Maximum resolution	2.06 Å	
Rotation axis	c^*	
Rotation range	180°	
Rotation step	2°/frame	
R_{merge}	0.08	0.13
No of independent reflections	36,788	22,523
Greater than 4σ		14,769
Completeness	76%	81.5%
Refinement resolution		20-2 Å
R value=0.146/0.175 for 4σ/all reflections (13,756/19,801)		
R_{free} (*24*)=0.206/0.234 for 4σ/all reflections (1,529/2,200)		
No of protein atoms		2,487
No of water molecules		223
Average B value for molecule a		28.9 Å²
molecule b		30.4 Å²
molecule c		29.3 Å²
water molecules		45.0 Å²
rms deviation from ideal distances		0.015 Å
Absolute error by method of Luzatti (*25*)		0.24 Å

TABLE II. **Amino acid sequences of proteins Bre, Roy, and Rei.**

Protein Roy: space group $P6_122$ a=81.8 Å, c=79.1 Å
Protein Rei: space group $P6_1$ a=75.8 Å, c=98.2 Å

BRE: DIQMTQSPSS LSASVGDRVT ITCQASQDIS DYLI WYQQKL GKAPNLLIYD ASTLETGVPS RFSGSGSGTE YTFTISSLQP EDIATYYCQQ YDDLPYTFGQ GTKVEI K
ROY: DIQMTQSPSS LSASVGDRVT ITCQASQDIS I FLNWYQQKP GKAPKLLIYD ASTLEAGVPS RFSGSGSGTD FTFTISGLQP EDIATYYCQQ FDNLPLTFGG GTKVDFKR
REI: DIQMTQSPSS LSASVGDRVT ITCQASQDII KYLNWYQQTP GKAPKLLIYE ASNLQAGVPS RFSGSGSGTD YTFTISSLQP EDIATYYCQQ YQSLPYTFGQ GTKLQI TR

monoclinic, giving an R_{merge} of 8%. It was only later discovered that the data could be indexed as orthorhombic with an R_{merge} of 12%. Details of the data collection and refinement are given in Table I.

Structure Determination—The dimer unit of proteins Roy (*16*) or Rei (*17*) which have similar cell dimensions, although different symmetry (Roy: $P6_122$, $a=b=81.8$ Å, $c=79.1$ Å, and Rei: $P6_1$, $a=b=75.8$ Å, $c=98.2$ Å) provided a successful starting point for the structure determination. The dimer was used for a molecular replacement search on the monoclinic indexing using the program X-PLOR (*18*). Three successful matches approximately 60° apart were found, corresponding to the three dimers in the asymmetric unit. The relationship between these three dimers was found by adjusting the distances up the screw axis and distances from the axis of the screw. The screw axis then completes 12 molecules in a single turn of the spiral which surrounds a rod of water 50 Å in diameter. There are two spirals in the unit cell running up the z axis, one coming up from the origin and the second from 1/2, 1/2, 0. Each spiral interacts and shares monomers with six neighboring spirals. In each monomer, 107 amino acid residues were clearly visible and identifiable by their shape.

Refinement—The structure was refined by the program Prolsq (*19*) together with model rebuilding using the program FRODO (*20*) with the conventional R value going to 0.19. The relationship to the orthorhombic symmetry was then discovered, and the structure was re-indexed. Refinement on the three monomers in the asymmetric unit of the orthorhombic setting by Prolsq reduced the R value to 0.18. When the research project was relocated at the National Sun Yat-sen University, the refinement was taken up using the program Shelxl97 (*21*) with model rebuilding using the program XtalView (*22*). A reexamination of the structure revealed no disagreement with the peptide atoms, but several of the side chains and most of the water molecules were changed. Using refinement with diffuse water scattering and a single over-all anisotropic temperature factor, the R value dropped to 0.14 with $R_{free}=0.20$ (*24*). The difference electron density map became more useful and several side chains were edited to improve poor dihedral angles or to allow hydrogen bonding. The three molecules in the asymmetric unit of the orthorhombic indexing are designated *a*, *b*, and *c*, each with residues 1-107.

RESULTS

The structure can best be described as hollow cylinders of protein with a central core of water that extend through the crystal in the z direction. Each cylinder contains 24 protein monomers in the repeat unit. The wall of each cylinder is fused with the walls of six surrounding cylinders which share 12 of the monomers. The other 12 monomers form a continuous spiral in the z direction.

Secondary and Tertiary Structure of the Monomer—The protein monomer consists of ten β-chains, A-J, and the connecting loops arranged in two β-sheets, ACHG and BJIDEF. The arrangement is classified as a beta barrel, but is more descriptively called a beta sandwich. Figure 1 is a stereo color drawing of the strands of the monomer. The numbering of the amino acid residues in the β-chains is given in Table III, as well as the color code for Fig. 1. All

TABLE III.

Contents of the four strands of the first sheet: ACHG; and the six strands of the second sheet: BJICEF. The color code is used in Fig 1.

	strand A	strand C	strand H	strand G	
	2	25	70	67	
	⇓	⇑	⇓	⇑	
	7	18	75	61	
	purple	blue	red-orange	orange	
strand B	strand J	strand I	strand D	strand E	strand F
8	96	90	32	50	52
⇓	⇓	⇑	⇓	⇑	⇓
13	107	85	38	45	55
purple	magenta	red	violet	green-blue	green

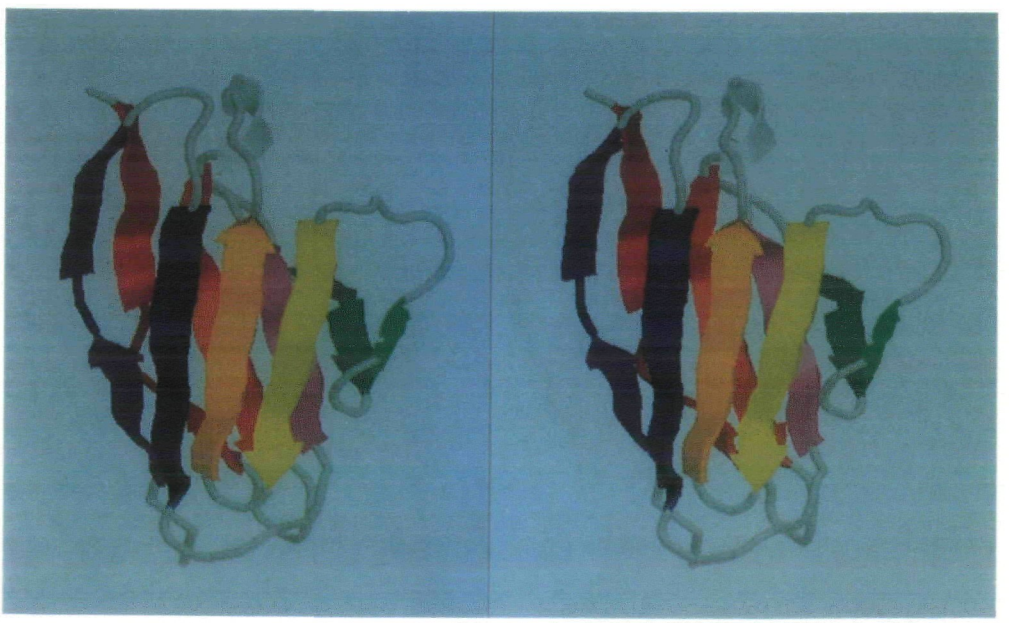

Fig. 1. **Stereo and colored view of the kappa monomer.** The residues corresponding to the colors are given in Table III. All β-strands are given a different color except that strands a and b are both purple. Figures 1, 5, and 6 were produced by the program RasWin from Glaxowellcome, Oxford, UK. Other figures were produced by XtalView.

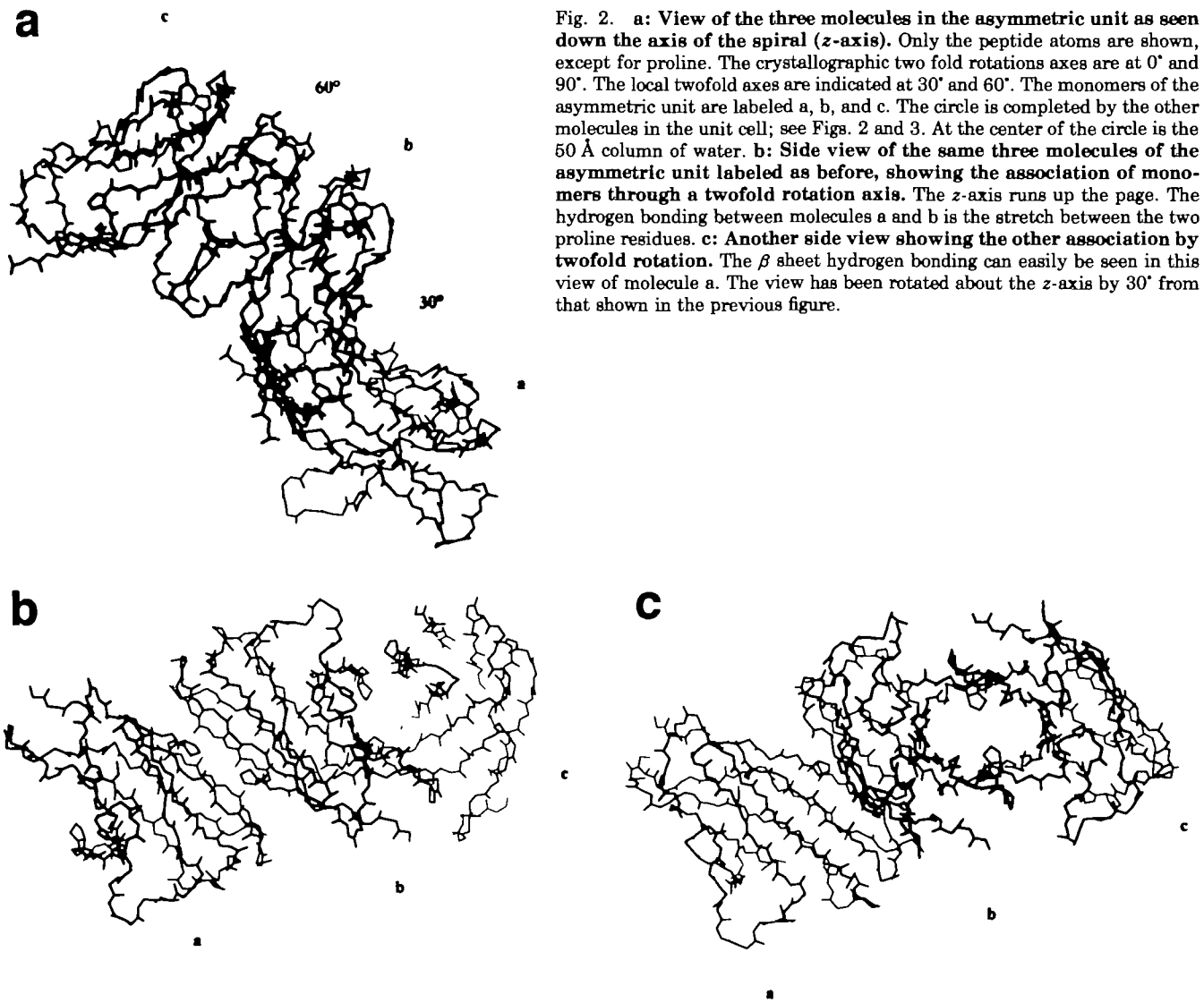

Fig. 2. **a: View of the three molecules in the asymmetric unit as seen down the axis of the spiral (*z*-axis).** Only the peptide atoms are shown, except for proline. The crystallographic two fold rotations axes are at 0° and 90°. The local twofold axes are indicated at 30° and 60°. The monomers of the asymmetric unit are labeled a, b, and c. The circle is completed by the other molecules in the unit cell; see Figs. 2 and 3. At the center of the circle is the 50 Å column of water. **b: Side view of the same three molecules of the asymmetric unit labeled as before, showing the association of monomers through a twofold rotation axis.** The *z*-axis runs up the page. The hydrogen bonding between molecules a and b is the stretch between the two proline residues. **c: Another side view showing the other association by twofold rotation.** The β sheet hydrogen bonding can easily be seen in this view of molecule a. The view has been rotated about the *z*-axis by 30° from that shown in the previous figure.

contacts between the β-chains are antiparallel, except for the B to J contact, which is parallel. A single disulfide link connects C to J. The loops between strands are not of uniform length, some are long, some are short, but all result in a reversal of direction of the polypeptide chain. Again, the one exception is the A to B loop, which moves from ACHG to BHIDEF without changing direction. The 10 β-strands, arranged in two levels, of each of the three monomers of the asymmetric unit, are shown in Fig. 2, a, b, and c, which are drawn using only the peptide atoms. The conformations of the three independent molecules in the asymmetric unit are almost identical, differing only in the rotations about some of the larger amino acid residues.

Quaternary Structure along the Spiral—As the 12 molecules go along to complete one turn of the spiral, each monomer makes contact to the next by twofold rotational symmetry perpendicular to the axis of the spiral. The sequence of the 12 monomers of the spiral would be

a b c ( ) c b a ( ) a b c ( ) c b a ( )

with ( ) denoting where the twofold rotation axes are used by the crystallographic symmetry. To help visualize the symmetry, imagine a line of automobiles parked on a spiral ramp with every second car facing the reverse direction and turned up-side-down.

There must be two interactions between monomers. The connections are not head to tail, but rather should be called head to head/tail to tail. The only true contact is along the path of the spiral. The molecules make contact with the next molecule up the spiral axis through a thin layer of water.

The site of the more regular of the two contacts is on the B strand, purple in Fig. 1, making β-sheet hydrogen bonds with the twofold related B strand of the next molecule along the spiral. There is extensive hydrogen bonding between the B strand of molecule a and the symmetry related strand of molecule b. Residues Ser9, Ser10, and Ser12 make peptide hydrogen bonds plus the OG atoms are involved between Ser10 and Ser12, and are strongly conserved, while Pro8, which precipitated the transition from the A strand to the B strand, is absolutely conserved. This contact should be relatively insensitive to the amino acid composi-

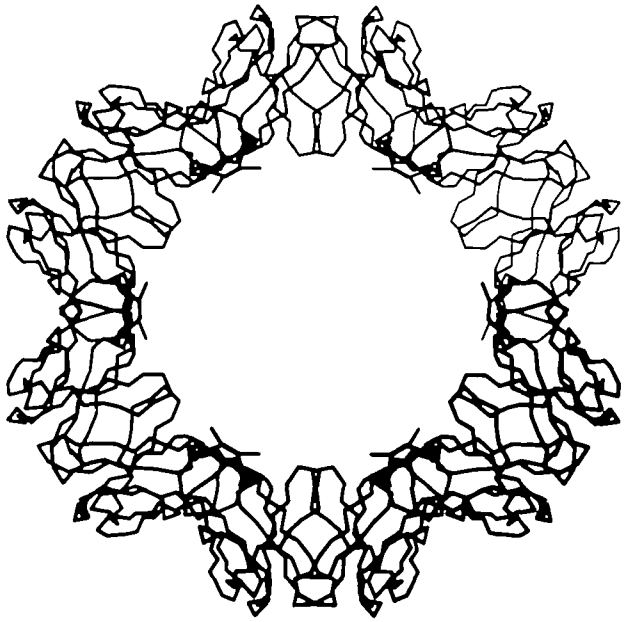

Fig. 3. **The view looking down the *z*-axis, showing all the 12 molecules in one turn of the spiral.** Only the trace of the α-carbon atoms is now shown. The inner diameter is 50 Å, the outer diameter 110 Å (including side chains), which is similar to the 70-100 Å diameter found for amyloid fibrils (4) by electron microscopy.

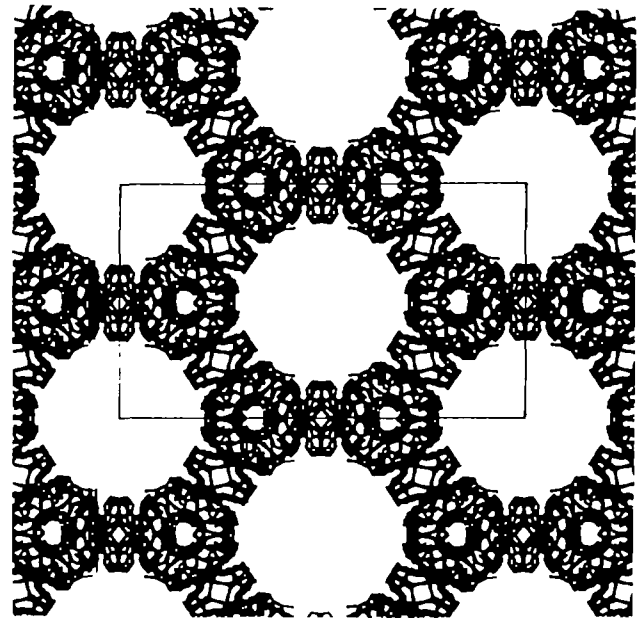

Fig. 4. **The same view as Fig. 3, only with all molecules of the cell, showing how the spirals interlock with each other.** The unit cell is drawn in.

tion of the strand, since only the peptide atoms are needed in the hydrogen bonding. Figure 2a shows molecules a, b, and c with the spiral axis, the *z* axis, coming up toward the viewer. The local twofold rotation axis between molecule a and molecule b is seen in Fig. 2a at the angle of 30°, for which the twofold axis is in the plane of the paper, and in Fig. 2b, in which the twofold axis is perpendicular to the paper.

The other contact, found between the b and c molecules, is through side chains only, involving the side chains of the I strand and the I-J loop, red and white, and the D-E loop, violet to blue-green. Contacts between the side chains of invariant residues Gln39 to Gln39 in the next monomer, and Gln89 to Gln89 in the neighbor are always present, while Gln89 to the neighboring Tyr36 and its reverse are usually present. A hydrophobic contact between Phe98 and the neighboring Pro40, and the reverse, is also found. These contacts are from the β-strand loops (D-E and I-J), which stick out like wings from the lower level sheet. This contact is around a twofold rotation axis as seen in Fig. 2a at 60°, and in Fig. 2c. The side chains most involved, Tyr36, Gln38, Lys42, Pro44, Gln89, and Phe98, are invariant residues. This contact is also found in the crystal structure of the non-amyloid protein Rei (*17*) and other light chain fragments. However, for each protein the contacts are at different angles, resulting in different crystal forms.

These kinds of contact are, in fact, quite similar to the contacts made by the tetramer of transthyretin, in which the β-sheet contact is more extensive and the contact of the wings is more tenuous. Therefore, we might suggest that the contacts in the fibril polymer might contain (at least) these two kinds of monomer to monomer associations, and that conditions which would favor such associations would favor fibril formation.

The Crystallographic Spiral—While protein crystals are usually described as "protein molecules, surrounded by water, and making contact with each nearest neighbors by only one or two residues," this crystal is a rod of water 50 Å in diameter that is surrounded by interlocking spirals of protein molecules. A view down the axis of the spiral (the *z*-axis) is given in Fig. 2a. Nine more molecules would be required to complete the spiral. As the spiral turns counterclockwise, the molecules advance toward the viewer. The final molecule has advanced 77.56 Å, which is twice the width of a single molecule. This space is filled by a molecule from a neighboring spiral, which interlocks with it much like the teeth of two worm gears can interlock with each other. Thus each turn of the spiral requires 12 other molecules to fill the space in between. Two molecules are contributed by each of the six neighboring spirals. Therefore, each turn of the spiral contains 24 molecules, in two strands, with one strand being continuous, and the other strand having contributions from six neighboring spirals. A view down the axis of the spiral using only the 12 molecules of the continuous spiral is given in Fig. 3. All atoms of the molecules are shown here. The identical view, but now showing the interlocking of the neighboring spirals, is given in Fig. 4.

DISCUSSION

The similarities between this crystal structure and the characteristics of the amyloid fibrils are obvious. However, it is not realistic to assume that the 12 molecule spiral would be a stable structure on its own. Figure 5 shows that the 12 molecules in the spiral fill only half the space. The other spaces come from the intersecting neighbors, which was shown in Fig. 4. However, in the amyloid fibril here is no evidence of interlocking spirals. If the spiral is to be a model for the fibril, these spaces must be filled, and the

neighbors will not be there in the fibril, since the fibrils have thickness only about the same as that of a single spiral.

The Double Spiral—Each spiral of 12 molecules is surrounded by 6 interlocking spirals, each contributing 2 molecules to fill the spaces in the first spiral to give 24 molecules in all. The neighboring spirals would not be present in the fibril, and one convenient way to fill the spaces caused by removing the interlocking spirals is to propose that the fibril is composed of a double spiral, with the second spiral having the same center, but rotated by 180°. A model of this can be conveniently generated using one of the familiar strategies of protein crystallography.

The 12 monomers in one repeat of the spiral are positioned in an large artificial unit cell of space group $P2$, with dimensions $a=200$ Å, $b=200$ Å, $c=77.56$ Å, gamma$=90°$, and with the c-axis being the same as that of the orthorhombic crystal. Figure 5 shows the 12-unit spiral when isolated. This spiral is unsupported by any contributions from neighbors and would be therefore unstable throughout its length. However, the contributions that were made by the neighbors can also be obtained from a second, companion spiral, such as is automatically generat-

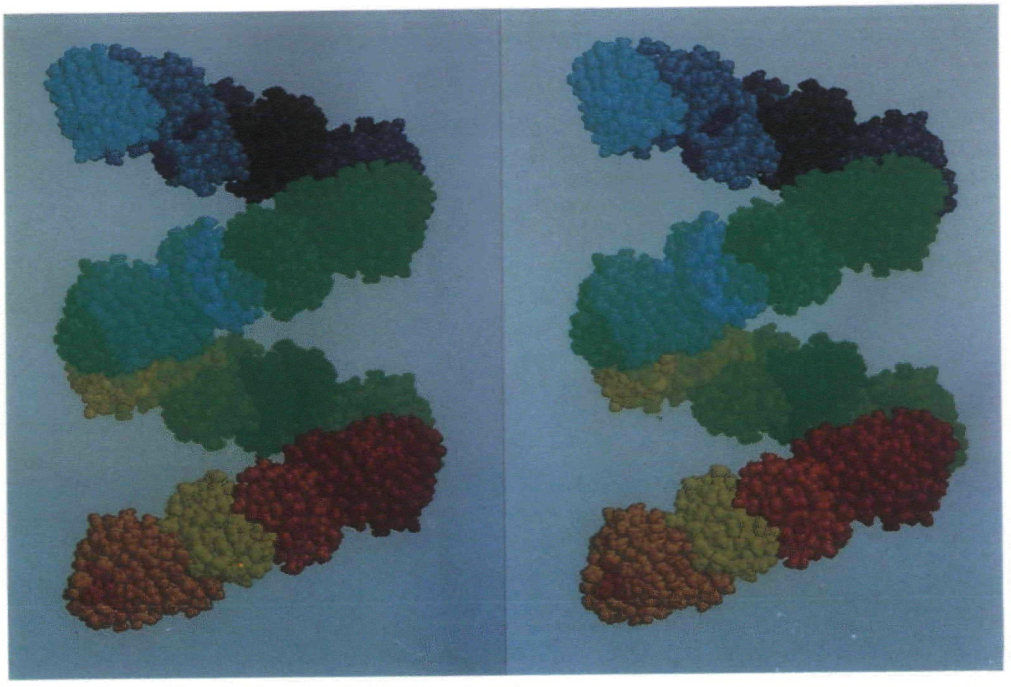

Fig. 5. **Side view in stereo and color of the single, isolated spiral of the crystal structure with the interlocking neighbors removed.** Each monomer is given a different color. The z-axis is vertical.

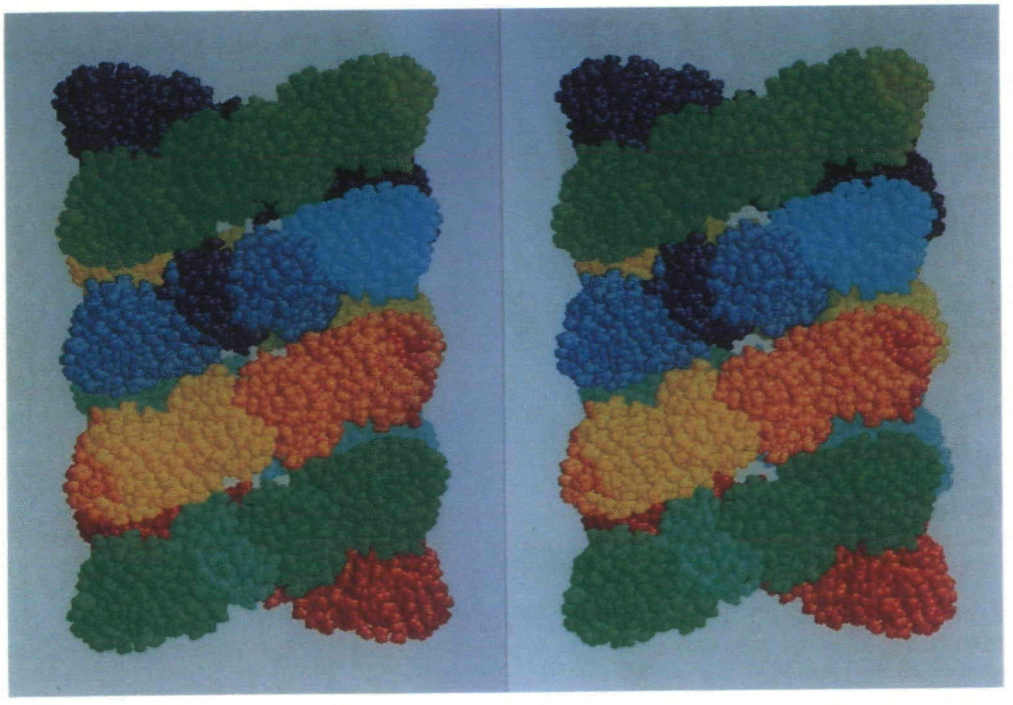

Fig. 6. **The same view in stereo and color, except that the vacant groove has been filled by another spiral having been rotated through 180°.** The original spiral may be found by comparison to Fig. 5, except that the colors are different.

ed by the twofold axis of the space group, $P2$. The inclusion of this is shown in Fig. 6. If the crystallographic symmetry were to be relaxed, there are some variables that could be used to optimize the fitting of the companion spiral. Among these are the starting point and the angle at which the lower sheets make contact. The double spiral should be stable except at each end.

In the fibril, there would be no crystallographic symmetry and the repeat distance of the spiral need not be the same as in the crystal and indeed need not be constant. The thin layer of water between the spirals would probably be variable, thus allowing a gentle twist or wobble in the course of the spiral. Moreover, occasional mistakes in the placement of the monomers may produce a loop of spiral that is external to the principal course of the spiral, thus resulting in a bulge along the course of the spiral.

The formation of fibril would be dependent on at least two factors, the stability and concentration of the native protein, and the stability of the protein in the fibril. For the double spiral model, a third factor needs to be considered, the central core.

The Central Core—The central column of water in this crystal structure is relatively featureless but is large enough to accommodate molecules of, as an example, another protein. Congo red dye has been observed to form intensely colored crystals with variants of TTR (*23*) and there would be room for several molecules of the dye in the unit cell. In the fibril the central core of the double spiral would have to be filled with something. It is appropriate to ask whether the double spiral could have a functional as well as a structural significance. One can speculate that fibril initiators may exist which would start the fibril that would then grow independently. Such an initiator would need be present only in very small amounts and would be difficult to detect. The fibril might be terminated or inhibited by similar mechanisms. Since other amyloidogenic proteins would have different double spiral dimensions and different amino acid compositions for the inner wall, the initiator would probably be different, and would not be common to all amyloid fibrils. An initiator could possible account for the late onset character of amyloidosis.

Similarity to Transthyretin—There are striking similarities between the Bre protein and transthyretin. Many amyloidogenic mutants of TTR are found, and the sites are widely spaced along the molecule. Both Bre and TTR are double β-sheet proteins with long stretches of antiparallel β-strands. Both form strong dimers through extensive hydrogen bonding along the edge of the β-sheet. The dimers of both form much weaker interactions to form the spiral in the case of Bre and to form the tetramer in the case of TTR (*10-14*). It can be assumed that TTR might well form a spiral structure in the fibril. The longer loops connecting the strands in TTR offer possibilities of interactions between the molecules in a spiral. This type of tetramer to spiral transition may have already been observed in the comparison of the structures of light chain dimers Wat and of Rei, which are of very similar amino acid composition. The quaternary structure of Rei is a spiral (*17*), while that of Wat is described by Huang *et al.* (*26*) as a tetramer.

It is hoped that the model proposed might suggest new ways of designing experiments about the chemical and physical properties of fibrils, and to suggest alternative ways of interpreting existing data. More information about the molecular structure of amyloid fibrils is necessary in order to produce procedures to stop, or to prevent, or to reverse the progress of amyloidosis. It is appropriate to speculate on some of the possible consequences of the proposed model. Let us use transthyretin as an example. During the formation of amyloid, there must be some kind of equilibrium between the tetramer form of TTR and the long polymer form. As mentioned before the TTR form a strong dimer and a weaker tetramer. The dimer has extensive β-sheet hydrogen bonding, yet has residues of the same charge facing each other, which opens the possibility of creating more stable forms of TTR. If yet another form of TTR monomer could be introduced into the blood that would form a more stable mixed tetramer with the mutant TTR than the mutant TTR forms with itself, then the equilibrium would be shifted toward the tetramer and away from the long polymer of the fibril, thereby reducing the formation of new fibrils and perhaps even removing existing fibrils.

Molecular modeling by computer graphics of the double spiral for the light chain proteins and for transthyretin should be a fruitful avenue of investigation, and has been initiated here.

In summary, we have presented the structure of the $\varkappa$ I protein Bre after refinement at 2.0 Å resolution. The monomers are connected together in a head to head/tail to tail arrangement in an infinite spiral with 12 molecules in the repeat. The monomers are not in contact with the next turn of the spiral, rather, there is another monomer in between. These monomers between come from neighboring spirals. Since the fibrils appear to have the dimensions of a single spiral, the spaces between must come from another source. It is therefore proposed that a simple model for the fibril would be a double spiral of two concentric spirals of 12 monomers each in the repeat. It is suggested that the cylinder of water at the center of the spiral could be the site of a mechanism for controlling the initiation or termination of the fibril. The similarities of the Bre structure and the crystal structure of transthyretin are presented, and it is suggested that transthyretin may form fibrils by a similar mechanism.

Crystallographic data for the orthorhombic form of Bre have been submitted to the Brookhaven protein data bank.

REFERENCES

1. Sipe, J.D. (1992) Amyloidosis. *Annu. Rev. Biochem.* **61**, 947-972
2. Bennhold, H. (1922) Eine spezifische Amyloidfärbung wit Kongorot. *Meunch. Med. Wocheschr.* **69**, 1537-1538
3. Divry, P. and Florkin, M. (1927) Sur les propriétés optiques de l'amyloïde. *c.r. soc. Belge biol.* **97**, 1808-1810
4. Cohen, A.S. and Calkins, E. (1959) Electron microscope observations on a fibrous component in amyloid of diverse origins. *Nature* **183**, 1202-1203
5. Eanes, E.D. and Glenner, G.G. (1968) X-ray diffraction studies on amyloid filaments. *J. Histochem. Cytochem.* **16**, 673-677
6. Termine, J.K., Eanes, E.D., Ein, D., and Glenner, G.G. (1972) Infra red spectroscopy of human amyloid fibrils and immuno globulin proteins. *Biopolymers* **11**, 1103-1113
7. Pas, M., Schubert, M., Zucker-Franklin, D., Rimon, A., and Franklin, E.C. (1968) Characterization of soluble amyloid prepared in water. *J. Clin. Invest.* **47**, 924
8. Costa, P.P., Figueira, A.S., and Bravo, F.R. (1978) Amyloid fibril protein related to prealbumin in familial amyloidotic polyneuropathy. *Proc. Natl. Acad. Sci. USA* **75**, 4499-4503

9. Blake, C.C.F., Geisow, J.J., Oatley, S.J., Rerat, B., and Rerat, C. (1978) Structure of prealbumin: Secondary, tertiary and quaternary interactions determined by Fourier refinement at 1.8 Å. *J. Mol. Biol.* **121**, 339-356
10. Hamilton, J.A., Steinrauf, L.K., Braden, B.C., Liepnieks, J., Benson, M.D., Holmgren, G., Sandgren, O., and Steen, L. (1993) The X-ray crystal structure refinements of normal human transthyretin and the amyloidogenic Val-30→Met variant to 1.7 Å resolution. *J. Biol. Chem.* **268**, 2416-2424
11. Hamilton, J.A., Steinrauf, L.K., Liepnieks, J., Benson, M.D., Holmgren, G., Sandgren, O., and Steen, L. (1992) Alternation in molecular structure which results in disease: The Met-30 variant of human plasma transthyretin. *Biochim. Biophys. Acta* **1139**, 9-16
12. Hamilton, J.A., Steinrauf, L.K., Braden, B.C., Murrell, J.R., and Benson, M.D. (1996) Structural changes in transthyretin produced by the Ile109Ser mutation which results in decreased affinity for retinol-binding protein. *Amyloid: int. J. Exp. Clin. Invest.* **3**, 1-12
13. Steinrauf, L.K., Hamilton, J.A., Braden, B.C., Murrell, J.R., and Benson, M.D. (1993) X-ray crystal structure of the Ala-109→Thr variant of human transthyretin which produces euthyroid hyperthyroxinemia. *J. Biol. Chem.* **268**, 2425-2430
14. Steinrauf, L.K., Hamilton, J.A., Clawson, D., Liepnieks, J., Murrell, J., and Benson, M. (1993) Structure of an immunoglobulin kappa variable light chain associated with primary amyloidosis. *Abstracts of the Annual Meeting of the American Crystallographic Association*, 128 (abstract PK17)
15. Schormann, N., Murrell, J.R., Liepnieks, J.J., and Benson, M.D. (1995) Tertiary structure of an amyloid immunoglobulin light chain protein: A proposed model for amyloid fibril formation. *Proc. Natl. Acad. Sci. USA* **92**, 9490-9494
16. Colman, P.M., Schramm, H.J., and Gurs, J.M. (1977) Crystal and molecular structure of the dimer of the variable domain of the Bence-Jones protein ROY. *J. Mol. Biol.* **116**, 73-79
17. Epp, O., Colman, P., Fehlhammer, H., Bode, W., Schiffer, M., Huber, R., and Palm, W. (1974) Crystal and molecular structure of a dimer composed of the variable portion of the Bence-Jones protein Rei. *Eur. J. Biochem.* **45**, 513-524
18. Brünger, A.T. (1992) *X-PLOR. Version 3.0. A System for X-Ray Crystallography and NMR*, Yale University Press, New Haven, CT
19. Hendrickson, W.A. (1985) Stereochemically restrained refinement of macromolecular structures. *Methods Enzymol.* **115**, 252-270
20. Jones, T.A. (1985) Diffraction methods for biological macromolecules. Interactive computer graphics: FRODO. *Methods Enzymol.* **115**, 157-171
21. Sheldrick, G. (1997) SHELXL: High-resolution refinement. *Methods Enzymol.* **277**, 319-343
22. McRee, D. (1998) *Practical Protein Crystallography*, Scripps Research Institute, La Jolla, California
23. Steinrauf, L.K., Cao, Y.J., Hamilton, J.K., Murrell, J., Liepnieks, J.J., and Benson, M.D. (1991) Preparation and crystallization of human transthyretin (prealbumin) variants. *Biochem. Biophys. Research Commun.* **179**, 804-809
24. Brünger, A.T. (1992) Free-R value: A novel statistical quantity for assessing the accuracy of crystal structures. *Nature* **355**, 472-475
25. Luzzati, V. (1952) Traitement statistique des erreurs dans la determination des structure cristallines. *Acta Cryst.* **5**, 802-810
26. Huang, D.-B., Chang, C.-H., Ainsworth, C., Brunger, A.T., Eulitz, M., Solomon, A., Stevens, F.J., and Schiffer, M. (1994) Comparison of crystal structures of two homologous proteins: structural origin of altered domain interactions in immunoglobulin light-chain dimers. *Biochemistry* **33**, 14848-14857